# Influences of Anisotropic Undrained Shear Strengths of Clays on Pullout Capacity of Planar Caissons

Suraparb Keawsawasvong[1,*], Jintara Lawongkerd[1,2]

[1]*Department of Civil Engineering, Thammasat School of Engineering, Thammasat University, Pathum Thani 12120, Thailand*
[2]*Department of Civil Engineering, Faculty of Engineering, Chulalongkorn University, Bangkok 10330, Thailand*

**ABSTRACT**

In this paper, the pullout capacity of planar suction caissons in anisotropic clays is investigated by the lower bound (LB) and upper bound (UB) finite element limit analysis (FELA), where Anisotropic Undrained Shear (AUS) failure criterion is associated with the analysis. The strengths of natural clays are conceivable to be anisotropic due to the characteristics of unequal shear strengths obtained from triaxial compression and extension tests. In the AUS failure criterion, there are three anisotropic undrained shear strengths obtained from triaxial compression, triaxial extension, and direct simple shear. Other failure criteria for ideal isotropic materials may be unfortunate to capture these anisotropic shear strengths since those models consider only a single undrained shear strength. New solutions of the pullout capacity of planar suction caissons in anisotropic clays are first-time derived based on three main dimensionless parameters, which are the ratio of depth to width of caissons, adhesion factor, and the ratio of undrained shear strength obtained from triaxial compression and triaxial extension. The pullout capacity factor affected by these parameters is also discussed in the paper to portray the influence of strength anisotropy of clays. The solutions to this problem can be used as design charts for general design purposes.

**Keywords:** Anisotropic clay; Finite element limit analysis; Plane strain; Pullout capacity; Suction caisson

## 1. Introduction

Floating offshore platforms are commonly supported by suction caissons, skirted foundations, or bucket foundations. Since these offshore platforms float on deep water due to the buoyant force, the foundations of these offshore platforms usually behave as anchored and mooring

---

**\*Corresponding author:** suraparb@hotmail.com

systems to resist the uplift force and maintain the positions of the platforms. The suction caisson is one of the famous types of offshore foundations that are made from reinforced concrete or steel. This foundation is constructed by sinking under its self-weight into the seabed. By pumping the water out from the inside of the caisson, the suction force is then developed at the interface between the caisson and the clay. An overview of the suction caisson can be found in the book by Randolph and Gourvenec [1].

There have been several studies on the capacity of suction caissons that employed field experiments (e.g. [2-3]) or centrifuge model tests (e.g. [4-5]). The numerical methods were also used to study the behavior of suction caissons. For example, Geer [6] and Whittle et al. [7] used finite element analysis to investigate the responses of suction caissons under axial loading. Another numerical method called finite element limit analysis (FELA) was used by various researchers to derive the solutions of the ultimate pullout load of suction caissons (e.g. [8-14]). Recently, Keawsawasvong and Ukritchon [15], Ukritchon, and Keawsawasvong [16] and Ukritchon et al. [17] presented the FELA solutions of the pullout capacity of suction caisson in isotropic clay.

Generally, natural clays exhibit some degree of strength anisotropy owing to their deposition and sedimentation processes resulting in preferred particle orientation as well as stress-induced anisotropy (e.g., [18, 19]). It should be recognized that the strengths and stiffnesses of soft clays are anisotropic, and depend on the orientation of depositional directions. The anisotropic undrained shear strengths of soft clays can be basically obtained from triaxial compression, triaxial extension, and direct simple shear, which can be represented by $S_{uc}$ (for compression), $S_{ue}$ (for extension), and $S_{us}$ (for simple shear), respectively. Note that these anisotropic undrained shear strengths are specifically a function of the plasticity index (PI) of clays as pointed out by Ladd [18]. Several previous works on regrading the stability problems associated with anisotropic strengths of clays have shown that the influences of anisotropic strengths of clays are significant (e.g. [20-27]). So far, the study on the pullout capacity of planar caissons in anisotropic clays has never been considered. Previous studies (e.g. [15-17]) considered only the pullout capacity of suction caissons in isotropic clays.

The objective of this paper is to investigate the influences of undrained shear strengths of anisotropic clays on the pullout capacity of planar suction caissons. In this paper, the new lower bound (LB) and upper bound (UB) solutions of the pullout capacity of planar caissons are numerically derived by using the finite element limit analysis (FELA). The FELA [28] is a computational method that combines the theorem of classical plasticity, the technique of numerical discretization using finite element, and a mathematical optimization that can be used to accurately predict the limit pullout load of suction caissons. The results from the present study can be applied to accurately and reliably estimate the pullout capacity of the planar caissons in which the effect of anisotropic undrained shear strengths are also taken into account.

## 2. Problem Definition

The problem definition of a planar suction caisson in an anisotropic clay under the plane strain condition is depicted in Fig. 1. Since the problem is axial-symmetric, only half of the domain is taken into account in the simulation, where the line of symmetry is defined to be located at the center of the caisson. A planar caisson with a depth $L$ and a width $B$ is subjected to ultimate pullout load $P$ and embedded in an anisotropic clay, where three anisotropic undrained shear strengths obtained from triaxial compression ($S_{uc}$), triaxial extension

($S_{ue}$), and direct simple shear ($S_{us}$) are taken into account. To specifically investigate the influence of the anisotropic shear strengths on the pullout capacity of the planar caisson under undrained conditions, the clay is defined as a weightless soil, where $\gamma$ is set to be zero so that the effect of unit weight does not interfere with the computed results.
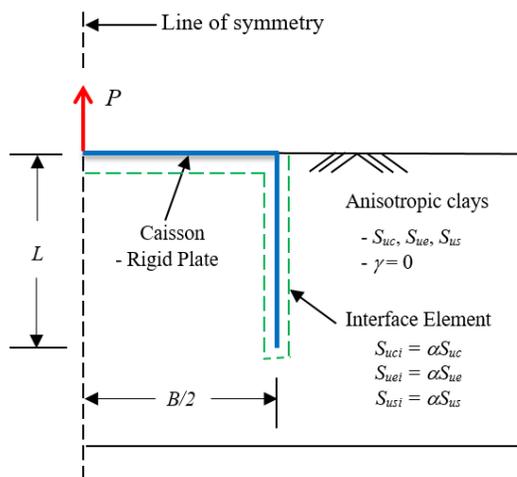


**Fig. 1.** Problem definition of planar caisson in anisotropic clay.

The strength at the soil-caisson interface has a strong impact on the pullout capacity of the suction caisson [15-17]. An adhesion factor, which controls the limiting shear strength at the interface, is also considered in this study and denoted by $\alpha$. The definition of the adhesion factor resulting in the reduction of three anisotropic shear strengths is shown below.

$$\alpha = \frac{S_{uci}}{S_{uc}} = \frac{S_{uei}}{S_{ue}} = \frac{S_{usi}}{S_{us}} \qquad (2.1)$$

where $S_{uci}$, $S_{uei}$, and $S_{usi}$ are the anisotropic undrained shear strengths at the interface. Note that the adhesion factor is in the range of 0 (smooth) – 1 (rough).

Based on [25, 26], the degree of undrained strength anisotropy of clays can be emphasized by introducing two anisotropic strength ratios $r_e$ and $r_s$. These anisotropic strength ratios can be expressed as the relations between three anisotropic shear strengths (e.g., $S_{uc}$, $S_{ue}$, $S_{us}$) as follows:

$$r_e = \frac{S_{ue}}{S_{uc}}, \qquad (2.2)$$

$$r_s = \frac{S_{us}}{S_{uc}}. \qquad (2.3)$$

As pointed out by Ladd [18], the undrained strength from the direct simple shear test seems to be slightly lower than the average value of the undrained strengths from the compression and extension tests. As a result, it is convenient to assume that there is a harmonic mean relation between $S_{uc}$, $S_{ue}$, and $S_{us}$ based on empirical data by Ladd [18], where the relationships of $S_{uc}$, $S_{ue}$, $S_{us}$, $r_e$, and $r_s$ can be expressed as:

$$S_{us} = \frac{2S_{ue}S_{uc}}{(S_{uc} + S_{ue})}, \qquad (2.4)$$

$$r_s = \frac{2r_e}{1 + r_e}. \qquad (2.5)$$

For the isotropic strength of clay, the above relations can be simply described as $r_e = 1$ and $r_s = 1$ (e.g., $S_{uc} = S_{ue} = S_{us}$), where the AUS failure criterion becomes the Tresca failure criterion.

The dimensionless technique [29] is employed to reduce the considered parameters in this study. It can be summarized that there are three dimensionless input parameters mainly resulting in the magnitude of the pullout capacity factor as follows:

$$\frac{P}{BS_{uc}} = f\left(\frac{L}{B}, \alpha, r_e\right), \qquad (2.6)$$

where $P/BS_{uc}$ denotes the pullout capacity factor; $L/B$ is the ratio of depth to width; $\alpha$

corresponds to adhesion factor; $r_e$ represents the ratio of undrained shear strengths obtained from triaxial compression and triaxial extension.

## 3. Method of Analysis

This paper applied LB and UB FELA techniques using the commercial software, namely OptumG2 [30], to derive the plastic solutions of the pullout capacity factor of planar caissons in anisotropic clays. The anisotropic soils are discretized into many triangular elements. Note that LB elements are three-noded elements with linear interpolation of unknown stresses, where stress discontinuity is allowed to occur at shared edges of adjacent elements. Besides, UB elements are six-noded elements that have quadratic interpolation of unknown displacements being continuous between elements. It should be noted that the true collapse load can be obtained by bracketing LB and UB solutions. The automatic mesh adaptivity with the default option of shear dissipation control is employed in the analyses to obtain more accurate LB and UB solutions. This function is one of the powerful functions in OptumG2. Krabbenhoft et al. [30] suggested that the setting of five adaptive steps of meshing with an initial mesh number of 5,000 elements that are automatically adapted and increased to a final mesh number of 10,000 elements is the best option to obtain accurate solutions, and still preserve the computational effort. Hence, this study applied this setting to all numerical models that are analyzed in the present study.

An anisotropic clay is modeled using the rigid-plastic material with the associated flow rule, where the AUS failure criterion is applied. The AUS model is a failure criterion for an anisotropic clay under the undrained condition that is available in OptumG2. The input strength parameters for the ASU model are $S_{uc}$, $r_e$, and $r_s$. More details regarding AUS model can be found in [31]. The unlimited tensile capacity is

assumed at the soil-structure interface (i.e., full-tension interface) to generate the fully developed suction force between the cap of the caisson and the underlying soil. A planar caisson is modeled using rigid plate elements. Both caisson and clay are assigned to be weightless materials. Besides, interface elements are set around the connection between the caisson and the clay. The numerical model of this problem in OptumG2 is shown in Fig. 2. The ultimate vertical pullout load $P$ is then computed by using the LB and UB FELA.
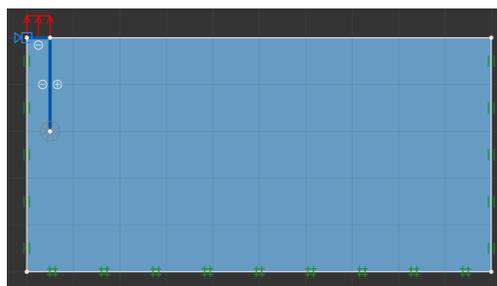


**Fig. 2.** A numerical model in OptumG2.

## 4. Results and Discussions

All numerical results obtained from LB and UB FELA are presented next. Note that the range of the ratio of depth to width $L/B$ is 1 to 6, and the range of the adhesion factor $\alpha$ corresponds to 0 to 1. These ranges are the practical values that can be generally found in practice. Besides, Krabbenhoft et al. [30, 31] suggested that the range of $r_e$ is about 0.5 to 1. Thus, these ranges are used as the scope of this present study. All the presented solutions proposed in this paper are the average solutions obtained from LB and UB solutions. In all cases, the exact pullout capacity factors can be accurately bracketed within 1% difference between the LB and UB solutions.
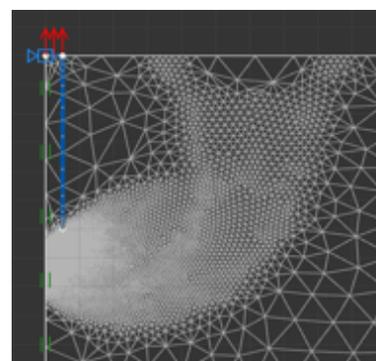
Examples of planar caissons under the ultimate pullout load after five adaptive steps are shown in Figs. 3(a) and 3(b) for the cases of $\alpha = 0.4$, $r_e = 0.7$, and $L/B = 1$ and 6, respectively. It can be seen from Fig. 3 that the number of meshes extraordinarily

increase in the zones containing high plastic shearing strain. This mesh adaptivity technique gives rise to more accurate results from LB and UB analyses. It can be implied that all simulations in the present study certainly reach the very accurate values of the pullout capacity factors.

All numerical results of the planar caissons in anisotropic clays are presented in Figs. 4(a), 4(b), 4(c), 4(d), 4(e), and 4(f) corresponding to the different values of $\alpha =$ 0, 0.2, 0.4, 0.6, 0.8, and 10, respectively. In Fig. 4, the non-linear relationships between $P/BS_{uc}$ and $L/B$ can be clearly seen. Note the contour lines in Fig. 4 represent constant values of $r_e$ varying from 0.5 to 1. It is found that an increase of $L/B$ causes an increase of $P/BS_{uc}$. Besides, an increase of $r_e$ about 0.2 results in an increase of $P/BS_{uc}$ around 5 to 12%. The presented solutions in Figs. 4(a) to 4(f) can be employed in the design process of the suction caisson in undrained clay, where an anisotropy effect of anisotropic clay is considered. The relationship between $P/BS_{uc}$ and $\alpha$ is demonstrated in Fig. 5 for the cases of $r_e =$ 0.5. It can be seen from Fig. 5 that the relationship between $P/BS_{uc}$ and $\alpha$ is linear when $L/B$ is larger, but the degree of nonlinearity becomes higher when $L/B$ decreases. In addition, the slopes of contour lines for the cases with larger $L/B$ are higher than that of a small one. Finally, Fig. 5 demonstrates the relationship between $P/BS_{uc}$ and $r_e$ for the cases of $L/B = 6$. It is found that the effect of $r_e$ on the relationship between $P/BS_{uc}$ and $r_e$ is non-linear. Clearly, a larger $r_e$ value produces a higher magnitude of pullout capacity factor. The presented solutions of the planar suction caissons in anisotropic clays can be extensively employed to predict the pullout capacity factor for practical design purposes.
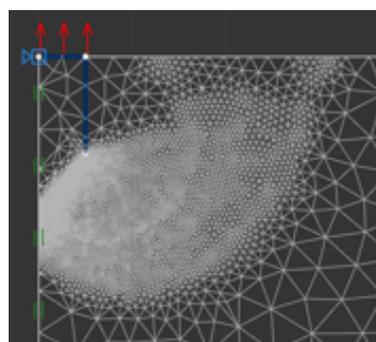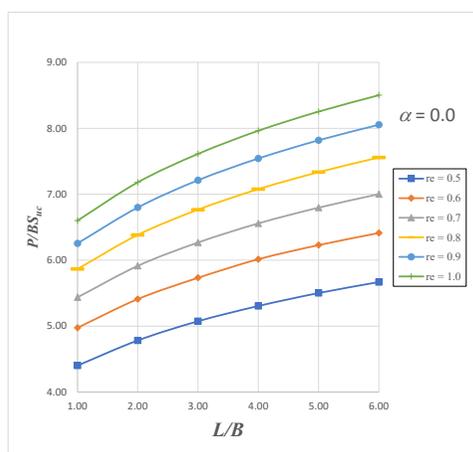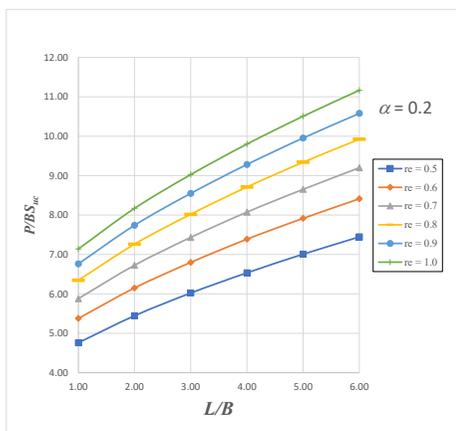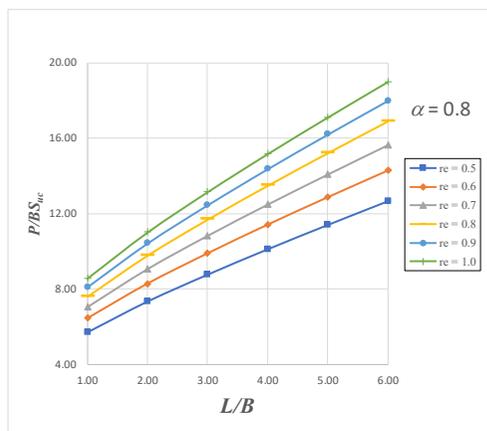


(a)



(b)

**Fig. 3.** Examples of planar caissons under ultimate pullout load after five adaptive meshings: (a) shallow caisson with $L/B = 1$, and (b) deep caisson with $L/B = 6$.
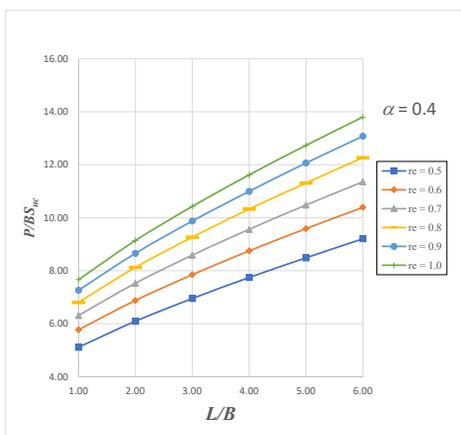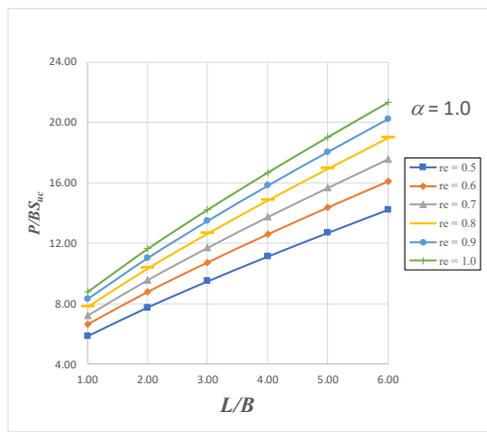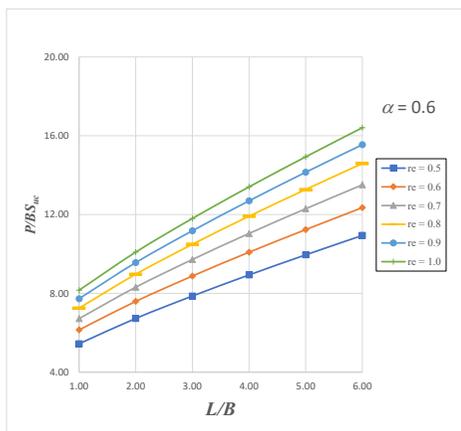


(a)

(b)



(e)



(c)



(f)

**Fig. 4.** Relationship between $P/BS_{uc}$ and $L/B$: (a) $\alpha = 0$, (b) $\alpha = 0.2$, (c) $\alpha = 0.4$, (d) $\alpha = 0.6$, (e) $\alpha = 0.8$, and (f) $\alpha = 1$.
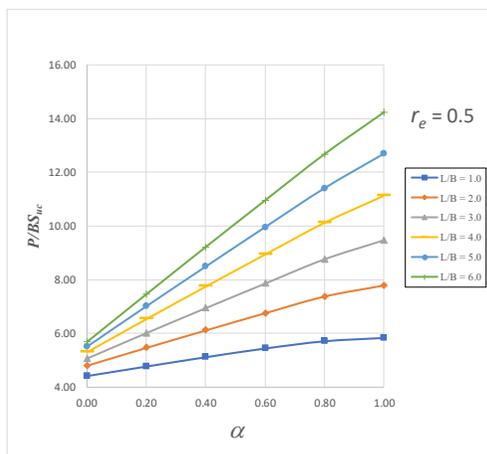


(d)



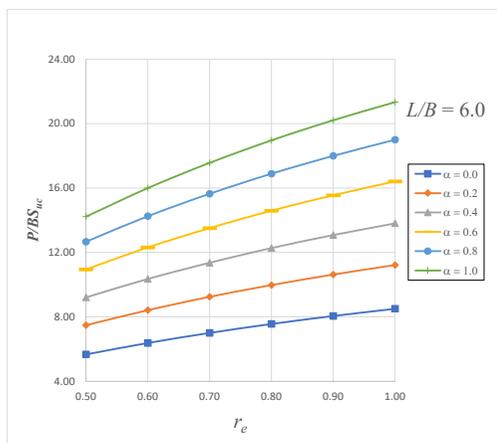**Fig. 5.** Relationship between $P/BS_{uc}$ and $\alpha$, where $r_e = 0.5$.

95

**Fig. 6.** Relationship between $P/BS_{uc}$ and $r_e$, where $L/B = 6$.

## 5. Use of Design Charts

In order to apply the proposed design charts shown in Figs. 4(a) to 4(f) to find the depth of a planar caisson, the following input parameters are determined as the width of the planar caisson is $B = 5$ m; the undrained shear strengths from triaxial compression and extension are $S_{uc} = 4$ kPa and $S_{ue} = 3.2$ kPa, respectively; the adhesion factor at the soil-caisson interface is $\alpha = 0.6$. This planar caisson is subjected to the allowable pullout load $P_{all} = 120$ kN. The factor of safety is defined to be $FS = 2$ resulting in the ultimate pullout load being $P = FS \times P_{all} = 240$ kN. Thus, the dimensionless parameters of this problem can be calculated as: $P/BS_{uc} = 12$, $r_e = S_{ue}/S_{uc} = 0.8$ and $\alpha = 0.6$. Since the $\alpha$ value is 0.6, Fig. 4(d) is required to find the ratio of depth to width $L/B$. By searching in Fig. 4(d) based on the values of $P/BS_{uc} = 12$ and $r_e = 0.8$, it can be found that the value of $L/B$ is about 4. Hence, the depth of this planar caisson must be larger than $L = 4B = 20$ m.

## 6. Conclusion

This paper demonstrates the impact of anisotropic undrained shear strengths of soft clays on the pullout capacity of planar suction caissons. The UB and LB FELA techniques are employed to derive the pullout capacity factor of this problem, where the AUS failure criterion is employed. Three dimensionless parameters including the ratio of depth to width of caissons, adhesion factor, and the ratio of undrained shear strength obtained from triaxial compression and triaxial extension. The influences of these dimensionless parameters on the pullout capacity factor are illustrated and discussed. The design charts for this problem are also proposed for general design purposes. An example of the use of design charts is also demonstrated in the paper.

## References
[1] Randolph M, Gourvence S. Offshore geotechnical engineering. Spon Press: Taylor & Francis; 2011.

[2] Andersen KH, Dyvik R, Schroder K, Hansteen OE, Bysveen S. Field test of anchors in clay II: Predictions and interpretation. J Geotech Geoenviron Eng 1993;119:1532-49.

[3] Dyvik R, Andersen KH, Hansen SB, Christophersen HP. Field test of anchors in clay I: Description. J Geotech Geoenviron Eng 1993;119:1515-31.

[4] Clukey EC, Morrison MJ, A Centrifuge and analytical study to evaluate suction caissons for TLP applications in gulf of Mexico. Design and Performance of Deep Foundation ASCE 1993;141-56.

[5] Cauble DF. Experimental measurements for a model suction caisson [Ph.D. thesis]. USA: Massachusetts Institute of Technology; 1996.

[6] Geer M. Analysis of pile and suction caisson behavior in axial loading. [Ph.D.

thesis]. USA: Massachusetts Institute of Technology; 1996.

[7]   Whittle AJ, Germaine JT, Cauble DF. Behavior of suction caisson foundations. Final Report. Report Submit to MIT; 1996.

[8]   Bransby MF, Yun G. The undrained capacity of skirted strip foundations under combined loading. Géotechnique 2009;59(2):115-25.

[9]   Gourvenec S. Effect of embedment on the undrained capacity of shallow foundations under general loading. Géotechnique 2008;58(3):177-85.

[10]  Gourvenec S, Barnett S. Undrained failure envelope for skirted foundations under general loading. Géotechnique 2011;61(3):263-70.

[11]  Mana DSK, Gourvenec S, Randolph MF. A numerical study of the vertical bearing capacity of skirted foundations. Proc 2ⁿᵈ Int Symp on Frontiers in Offshore Geotechnics (ISFOG); 2010.

[12]  Mana DSK, Gourvenec S, Randolph MF, Hossain MS. Failure mechanisms of skirted foundations in uplift and compression. Int J Phys Modell Geotech 2012;12(2):47-62.

[13]  Yun G, Bransby MF. The undrained vertical bearing capacity of skirted foundations, Soils Found 2007;47(3): 493-505.

[14]  Mana DSK, Gourvenec S, Martin CM. Critical skirt spacing for shallow foundations under general loading. J Geotech Geoenviron Eng 2013;139:1554-66.

[15]  Keawsawasvong S, Ukritchon B. Finite element limit analysis of pullout capacity of planar caissons in clay. Comput Geotech 2016;75:12-7.

[16]  Ukritchon B, Keawsawasvong S. Undrained pullout capacity of cylindrical suction caissons by finite element limit

analysis. Comput Geotech 2016;80:301-11.

[17]  Ukritchon B, Wongtoythong P, Keawsawasvong S. New design equation for undrained pullout capacity of suction caissons considering combined effects of caisson aspect ratio, adhesion factor at interface, and linearly increasing strength. Appl Ocean Res 2018;75:1-14.

[18]  Ladd CC. Stability evaluations during stage construction. J Geotech Eng 1919;117(4):540-615.

[19]  Ladd CC, DeGroot DJ. Recommended practice for soft ground site characterization. In Proc 12ᵗʰ Panamerican Conference on Soil Mechanics and Geotechnical Engineering, Cambridge; 2003.

[20]  Davis EH, Christian JT. Bearing capacity of anisotropic cohesive soil. J Soil Mech Found Div 1971;97(5):753-69.

[21]  Su SF, Liao HJ, Lin YH. Base stability of deep excavation in anisotropic soft clay. J Geotech Geoenviron Eng 1998;124(9): 809-19.

[22]  Su SF, Liao HJ. Effect of strength anisotropy on undrained slope stability in clay. Geotechnique 1999;49(2):215-30.

[23]  Ukritchon B, Keawsawasvong S. Lower bound limit analysis of an anisotropic undrained strength criterion using second-order cone programming. Int J Numer Anal Methods Geomech 2018;42(8):1016-33.

[24]  Ukritchon B, Keawsawasvong S. Three-dimensional lower bound finite element limit analysis of an anisotropic undrained strength criterion using second-order cone programming. Comput Geotech 2019;106:327-44.

[25]  Ukritchon B, Keawsawasvong S. Lower bound solutions for undrained face stability of plane strain tunnel headings in

anisotropic and non-homogeneous clays. Comput Geotech 2019;112:204-17.

[26] Ukritchon B, Keawsawasvong S. Undrained stability of unlined square tunnels in clays with linearly increasing anisotropic shear strength. Geotech Geol Eng 2020;38(1):897-915.

[27] Ukritchon B, Keawsawasvong S. Undrained lower bound solutions for end bearing capacity of shallow circular piles in non-homogeneous and anisotropic clays. Int J Numer Anal Methods Geomech 2020;44(5):596-632.

[28] Sloan SW. Geotechnical stability analysis. Géotechnique 2013;63(7):531-72.

[29] Butterfield R. Dimensional analysis for geotechnical engineering. Géotechnique 1999;49(2):357-66.

[30] Krabbenhoft K, Lyamin A, Krabbenhoft J. Optum computational engineering (OptumG2) [cited 2020 Feb 01]. Available from: http://www.optumce.com

[31] Krabbenhoft K, Galindo-Torres SA, Zhang X, Krabbenhøft J. AUS: Anisotropic undrained shear strength model for clays. Int J Numer Anal Methods Geomech 2019;43(17):2652-66.